

**Yoshihiko Nakamura
Hideo Hanafusa
Tsuneo Yoshikawa**

Automation Research Laboratory
Kyoto University
Uji, Kyoto
611 Japan

Task-Priority Based Redundancy Control of Robot Manipulators

Abstract

In this paper, we describe a new scheme for redundancy control of robot manipulators. We introduce the concept of task priority in relation to the inverse kinematic problem of redundant robot manipulators. A required task is divided into subtasks according to the order of priority. We propose to determine the joint motions of robot manipulators so that subtasks with lower priority can be performed utilizing redundancy on subtasks with higher priority. This procedure is formulated using the pseudoinverses of Jacobian matrices. Most problems of redundancy utilization can be formulated in the framework of tasks with the order of priority. The results of numerical simulations and experiments show the effectiveness of the proposed redundancy control scheme.

1. Introduction

Robot manipulators have usually been designed to have no more than six degrees of freedom, which is the least degrees of freedom needed to perform 3-D tasks. Although six degrees of freedom are sufficient for conventional mechanical design, robot manipulators are expected to be more flexible and adaptive, like human arms. When a robot manipulator is required to trace a given trajectory of the end effector while avoiding obstacles in the workspace, more degrees of freedom are needed than in a free working space.

Whitney (1972) and Uchiyama (1979) pointed out that redundancy of a robot manipulator is effective for

overcoming its kinematical singularities. Redundancy is also effective for enabling a robot manipulator to approach a workpiece from all directions or to trace a given spatial trajectory avoiding obstacles in a workspace (Freund 1977). Whitney (1969, 1972) discussed the redundancy of prosthetic arms. Although he gave a criterion to minimize the integrated value of kinetic energy, he simplified it because of the large amount of computations and proposed to minimize the quadratic form of joint velocity instantaneously. This method implies the motion resolution by means of the weighted pseudoinverse of the full-rank Jacobian matrix. Nakano and Ozaki (1974), on the other hand, suggested *minimum potential energy criterion*, which forces a restriction on the inverse kinematics of an anthropomorphic manipulator so that the position of the elbow should be located in the vertical direction as low as possible. The criteria by Whitney and Nakano and Ozaki seem to be focused not on the active utilization of redundancy but on the unique determination of the solutions.

Liegeois (1977) discussed the active utilization of redundancy of robot manipulators. He expressed the general solution of joint velocity by means of the generalized inverse of the Jacobian matrix and proposed to determine the arbitrary vector as a gradient vector of a scalar function. He also showed the numerical simulation of utilizing redundancy for keeping the joint angles within their physical limitation. Hanafusa, Yoshikawa, and Nakamura (1978) proposed a numerical algorithm to plan a joint trajectory of a redundant manipulator using the general solution expressed by the pseudoinverse of the Jacobian matrix, where the limitation of joint angles and torques and the restriction imposed by obstacles were considered. Hanafusa, Yoshikawa, and Nakamura (1981) analyzed redundancy of robot manipulators in light of the matrix theory and discussed its utilization. Klein and Huang (1983) reviewed the control of redundant manipulators

by means of pseudoinverses, where they suggested a computational algorithm to reduce the computational amount. Moreover, Klein (1984) showed by numerical simulation that a manipulator can avoid an obstacle by paying attention to the point on the manipulator that is the shortest distance from the obstacle. Konstantinov, Markov, and Nenchev (1981) also discussed the utilization of redundancy for the physical limitation of joint angles by means of the pseudoinverse of the Jacobian matrix. Benati, Morasso, and Tagliasco (1982), on the other hand, proposed a recursive algorithm for inverse kinematics of an anthropomorphic redundant manipulator.

There are two possible approaches to the redundancy utilization problem: (1) instantaneously optimal control of redundancy and (2) globally optimal control of redundancy. Although the first approach requires a small amount of computation, it lacks a guarantee of global optimality. The second approach guarantees global optimality, but it requires a large amount of computation. Thus, the instantaneously optimal control approach is suitable for real-time redundancy control, such as sensor-based obstacle avoidance problems. The globally optimal control approach is better for off-line trajectory planning for tasks requiring strict optimality, such as obstacle avoidance problems in more complicated working spaces and energy minimizing problems. Therefore, these two approaches should be used properly according to the circumstances in which redundancy control is necessary.

In this paper, we will discuss the *instantaneously optimal control of redundancy*. To formulate the problem, the concept of task priority is introduced into kinematic inverse problems. A required task is divided into subtasks according to the order of priority. Then, the joint motions of robot manipulators are resolved in such a way that subtasks with lower priority are realized using redundancy or extra degrees of freedom not committed to satisfying subtask requirements of higher priority. This procedure is formulated based on the Jacobian matrix and its pseudoinverse. Although the basic idea was already published by the authors in Japanese (Hanafusa, Yoshikawa, and Nakamura 1983), this paper describes more complete formulations, including the dynamics of manipulators and the use of potential functions for obstacle avoidance and

also shows the new result of their simulations. In Section 3, we formulate the problem in the framework of *the resolved motion rate control* (Whitney 1969). Numerical simulations are carried out in Section 4 to show the effectiveness of the formulation, where the formulation is extended to the framework of *the resolved acceleration control* in order to consider the dynamics of manipulators (Luh, Walker, and Paul 1980). Two examples are simulated in Section 4: in one case, the position of the end effector is prior to the orientation; in the other case, the obstacle avoidance problem, where artificial potential function (Khatib and Le Maitre 1978), is used to describe the lower priority motion. In Section 5, experiments of obstacle avoidance are carried out on a robot manipulator with seven degrees of freedom to discuss the implementation and the actual effectiveness of the formulation. The information on obstacle is taught as a reference joint angle by an operator and used as the desired value of the lower priority task. Operator intervention of this kind would be a simple but effective method to utilize the global judgment of human operators in obstacle avoidance problems.

2. Tasks with the Order of Priority

We sometimes find tasks where the position or the orientation of the end effector is more important than the other. For example, in welding, cutting, and shape measurement, the position of the end effector is more important than the orientation. On the other hand, with spray painting, or directing a camera to objects, orientation is more important. We consider these tasks to be composed of subtasks with different levels of significance and call them *tasks with the order of priority*.

The usual problems of redundancy utilization can be formulated in the framework of tasks with the order of priority. When a redundant manipulator is required to trace a given trajectory of the end effector while avoiding obstacles in the workspace, trajectory tracing is given the first priority and obstacle avoidance is given the second priority. When a redundant manipulator is needed to trace a given trajectory of the end

effector while avoiding singular points, trajectory tracking is given the first priority and singularity avoidance is given the second priority.

For the tasks with the order of priority, if it is impossible to perform all of the subtasks completely because of the degeneracy or the shortage of degrees of freedom, it seems reasonable, then, to perform the most significant subtask preferentially and the less important subtasks (as well as possible) using the remaining degrees of freedom. In Section 3, the problem of redundancy utilization will be formulated based on this idea.

3. Inverse Kinematic Solutions Considering the Order of Priority

Here, to simplify the discussion, we formulate the problem for a case with two subtasks. This formulation can easily be extended to a case with more than two subtasks. The subtask with the first priority will be specified using the first manipulation variable, $\mathbf{r}_1 \in R^{m_1}$, and the subtask with the second priority will be specified using the second manipulation variable, $\mathbf{r}_2 \in R^{m_2}$. The kinematic relationships between the joint variable $\theta \in R^n$ and the manipulation variables are expressed as follows:

$$\mathbf{r}_i = \mathbf{f}_i(\theta), \quad (i = 1, 2) \quad (1)$$

Their differential relationships are expressed as follows:

$$\dot{\mathbf{r}}_i = \mathbf{J}_i(\theta)\dot{\theta}, \quad (i = 1, 2) \quad (2)$$

where $\mathbf{J}_i(\theta) \triangleq \partial \mathbf{f}_i / \partial \theta \in R^{m_i \times n}$ is the Jacobian matrix for the i th manipulation variable.

The general solution of Eq. (2) for $i = 1$ is obtained using pseudoinverses, as follows (Boullion and Odell 1971):

$$\dot{\theta} = \mathbf{J}_1^*(\theta)\dot{\mathbf{r}}_1 + (\mathbf{I} - \mathbf{J}_1^*(\theta)\mathbf{J}_1(\theta))\mathbf{y}, \quad (3)$$

where $\mathbf{J}_1^*(\theta) \in R^{n \times m_1}$ is the pseudoinverse of $\mathbf{J}_1(\theta)$ and $\mathbf{y} \in R^n$ is an arbitrary vector. If the exact solution does not exist, Eq. (3) represents the least-squares solution, minimizing $\|\dot{\mathbf{r}}_1 - \mathbf{J}_1(\theta)\dot{\theta}\|$.

Now, substituting Eq. (3) into Eq. (2) for $i = 2$, we get the following equation:

$$\mathbf{J}_2(\mathbf{I} - \mathbf{J}_1^*\mathbf{J}_1)\mathbf{y} = \dot{\mathbf{r}}_2 - \mathbf{J}_2\mathbf{J}_1^*\dot{\mathbf{r}}_1. \quad (4)$$

If the exact solution of \mathbf{y} exists for Eq. (4), it means that the second manipulation variable can be realized. However, the exact solution does not generally exist. We get \mathbf{y} , which minimizes $\|\dot{\mathbf{r}}_2 - \mathbf{J}_2(\theta)\dot{\theta}\|$, in the same way as Eq. (3). That is,

$$\mathbf{y} = \tilde{\mathbf{J}}_2^*(\dot{\mathbf{r}}_2 - \mathbf{J}_2\mathbf{J}_1^*\dot{\mathbf{r}}_1) + (\mathbf{I} - \tilde{\mathbf{J}}_2^*\tilde{\mathbf{J}}_2)\mathbf{z}, \quad (5)$$

where $\tilde{\mathbf{J}}_2 \triangleq \mathbf{J}_2(\mathbf{I} - \mathbf{J}_1^*\mathbf{J}_1)$, and $\mathbf{z} \in R^n$ is an arbitrary vector.

The solution $\dot{\theta}$ is obtained from Eqs. (3) and (5) as follows:

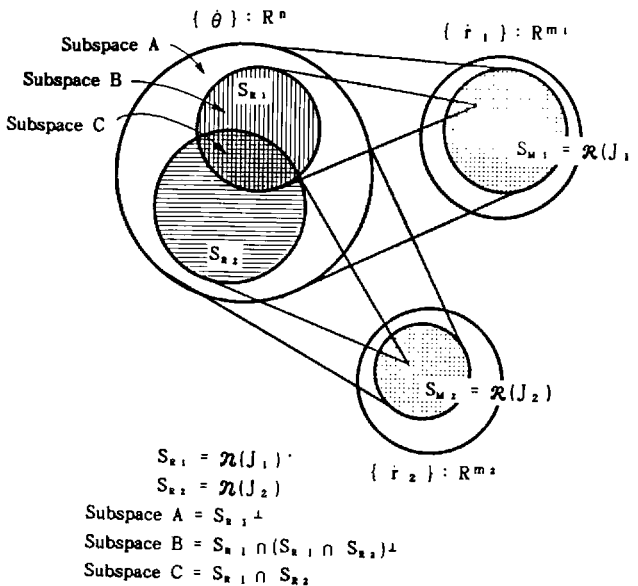
$$\dot{\theta} = \mathbf{J}_1^*\dot{\mathbf{r}}_1 + (\mathbf{I} - \mathbf{J}_1^*\mathbf{J}_1)\tilde{\mathbf{J}}_2^*(\dot{\mathbf{r}}_2 - \mathbf{J}_2\mathbf{J}_1^*\dot{\mathbf{r}}_1) + (\mathbf{I} - \mathbf{J}_1^*\mathbf{J}_1)(\mathbf{I} - \tilde{\mathbf{J}}_2^*\tilde{\mathbf{J}}_2)\mathbf{z}. \quad (6)$$

Equation (6) represents the inverse kinematic solution considering task priority.*

We defined the range space of the Jacobian matrix, $\mathcal{R}(\mathbf{J})$, as the manipulable space, and the null space of the Jacobian matrix, $\mathcal{N}(\mathbf{J})$, as the redundant space (Hanafusa, Yoshikawa, and Nakamura 1981). Figure 1 shows the general relationship between the manipulable spaces and the redundant spaces for the first and the second manipulation variables. In Fig. 1, Subspace A, Subspace B, and Subspace C are S_{R1}^\perp , $S_{R1} \cap (S_{R1} \cap S_{R2})^\perp$, and $S_{R1} \cap S_{R2}$ respectively, where $S_{R1} = \mathcal{N}(\mathbf{J}_1)$, $S_{R2} = \mathcal{N}(\mathbf{J}_2)$, and S_*^\perp means the orthogonal complement of subspace S_* . Subspace A means the contribution of $\dot{\theta}$ to the first manipulation variable. Subspace B can contribute to the second manipulation variable

* After submission of this paper, a paper by Maciejewski and Klein (1985) was published, which proved that the second term of Eq. (6) can be reduced to $\tilde{\mathbf{J}}_2^*(\dot{\mathbf{r}}_2 - \mathbf{J}_2\mathbf{J}_1^*\dot{\mathbf{r}}_1)$.

Fig. 1. Manipulable spaces and redundant spaces for the first and the second manipulation variables.



without disturbing the first manipulation variable. Subspace C means the remaining degrees of freedom and can be used for performing the third manipulation variable, if necessary. The first term in the right-hand side of Eq. (6) is the mapping of $\dot{\mathbf{r}}_1$ onto Subspace A. The second term means the mapping onto Subspace B of $\dot{\mathbf{r}}_2 - J_2 J_1^* \dot{\mathbf{r}}_1$, which is the desired value of the second manipulation variable modified considering the effect of the first term on the second manipulation variable. The third term is the orthogonal projection of the arbitrary vector \mathbf{z} onto Subspace C. If there is a third manipulation variable, an arbitrary vector \mathbf{z} is determined in the same way as \mathbf{y} .

In the case of $\mathbf{r}_2 = \theta$, Eq. (6) can be reduced to a simpler form using $J_2 = \mathbf{I}$ as follows:

$$\dot{\theta} = J_1^* \dot{\mathbf{r}}_1 + (\mathbf{I} - J_1^* J_1) \dot{\mathbf{r}}_2, \quad (7)$$

where the relationships of $(\mathbf{I} - \mathbf{M}^* \mathbf{M})^* = \mathbf{I} - \mathbf{M}^* \mathbf{M}$ and $(\mathbf{I} - \mathbf{M}^* \mathbf{M}) \cdot (\mathbf{I} - \mathbf{M}^* \mathbf{M}) = \mathbf{I} - \mathbf{M}^* \mathbf{M}$ are used. In Eq. (7), the term corresponding to the third term in Eq. (6) is equal to zero, which means that no degree of freedom remains for the third manipulation variable because the second manipulation variable $\mathbf{r}_2 = \theta$ requires all of the remaining degrees of freedom.

Fig. 2. 3 d.o.f. manipulator.

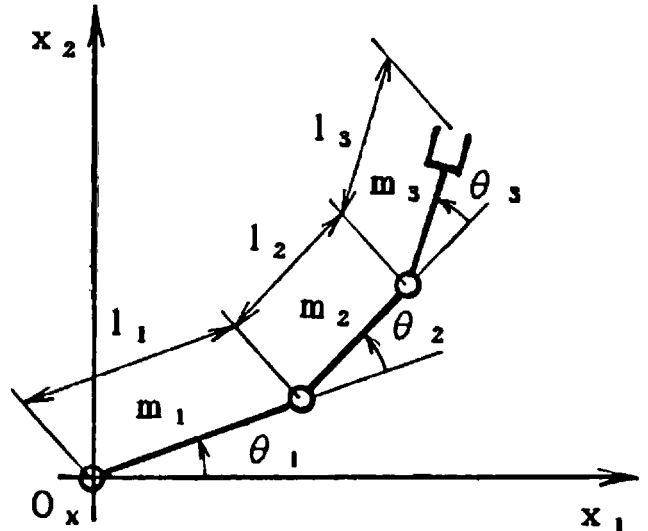


Table 1. Parameters of 3 d.o.f. Manipulator

i	l_i (cm)	m_i (kg)
1	50.0	30.0
2	43.3	25.0
3	35.0	20.0

4. Numerical Simulations

4.1. A Case in Which the Position of the End Effector is Prior to the Orientation

Here we perform a numerical simulation where the position of the end effector is prior to the orientation. Suppose that a robot manipulator has three degrees of freedom, as shown in Fig. 2. (The parameters of the manipulator are summarized in Table 1.) The mass of each link is distributed uniformly, and the manipulator is constrained within a horizontal plane. Therefore, the dynamics of the manipulator is represented as follows:

$$\mathbf{T} = \mathbf{A}(\theta) \ddot{\theta} + \mathbf{B}(\theta, \dot{\theta}), \quad (8)$$

Fig. 3. Simulation results where the position of the end effector is prior to the orientation.

where $T, \theta, \dot{\theta} \in R^3$, $A(\theta) \in R^{3 \times 3}$ is an inertia matrix, and $B(\theta, \dot{\theta}) \in R^3$ implies the effect of Coriolis and centrifugal forces.

The first and second manipulation variables are described as follows:

$$\mathbf{r}_1 = (x_1 \ x_2)^T, \quad (9)$$

$$r_2 = \cos(\theta_1 + \theta_2 + \theta_3), \quad (10)$$

where x_1 and x_2 are the position of the end effector in Cartesian coordinates and r_2 is the orientation of the end effector.

By differentiating Eq. (2) with respect to time, the following equation is derived:

$$\ddot{\mathbf{r}}_i = \mathbf{J}_i(\theta)\ddot{\theta} + \dot{\mathbf{J}}_i(\theta)\dot{\theta}. \quad (11)$$

A feedback control scheme is chosen so that the following equation may represent the closed-loop characteristics:

$$(\ddot{\mathbf{r}}_i^o(t) - \ddot{\mathbf{r}}_i) + G_{1,i}(\dot{\mathbf{r}}_i^o(t) - \dot{\mathbf{r}}_i) + G_{2,i}(\mathbf{r}_i^o(t) - \mathbf{r}_i) = 0, \quad (12)$$

where $\mathbf{r}_i^o(t)$ is the desired trajectory of the i th manipulation variable and $G_{1,i}$ and $G_{2,i}$ are the scalar feedback coefficients for the i th manipulation variable. If $G_{1,i}$ and $G_{2,i}$ are so chosen that Eq. (12) is stable, $\mathbf{r}_i(t)$ will converge to $\mathbf{r}_i^o(t)$. From Eqs. (11) and (12), the joint acceleration necessary to realize the feedback control scheme should satisfy the following equation:

$$\begin{aligned} \mathbf{J}_i(\theta)\ddot{\theta} &= -\dot{\mathbf{J}}_i(\theta)\dot{\theta} + \ddot{\mathbf{r}}_i^o(t) + G_{1,i}(\dot{\mathbf{r}}_i^o(t) - \dot{\mathbf{r}}_i) \\ &\quad + G_{2,i}(\mathbf{r}_i^o(t) - \mathbf{r}_i) \triangleq \mathbf{h}_i(\theta, \dot{\theta}, t). \end{aligned} \quad (13)$$

Since Eq. (13) is similar to Eq. (2), the approach discussed in Section 3 can be applied here. To simplify the computation, Eq. (7) was applied in place of Eq. (6) by solving Eq. (13) for $i = 2$ and regarding the solution $\ddot{\theta} = \mathbf{J}_2^* \mathbf{h}_2$ as the desired acceleration of the second manipulation variable. That is,

$$\ddot{\theta} = \mathbf{J}_1^* \mathbf{h}_1 + (\mathbf{I} - \mathbf{J}_1^* \mathbf{J}_1) \mathbf{J}_2^* \mathbf{h}_2. \quad (14)$$

The joint torque to be applied was calculated by substituting Eq. (14) into Eq. (8).

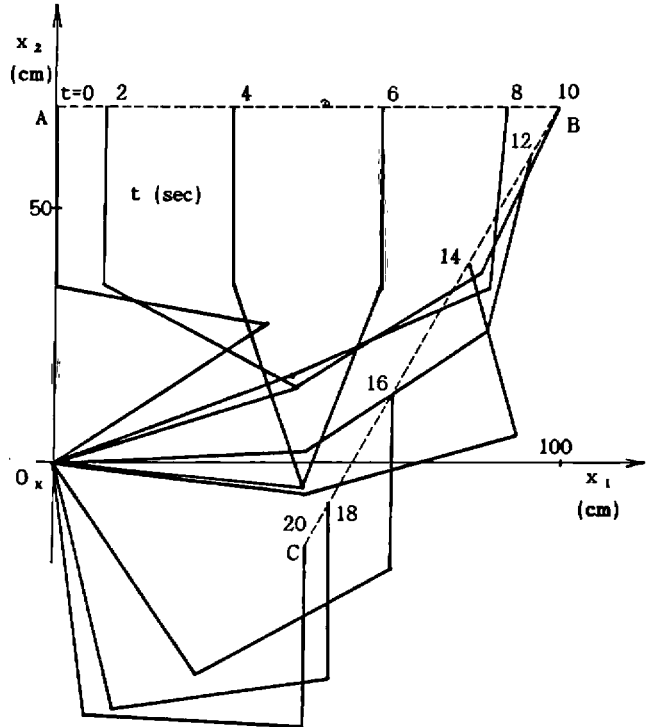


Figure 3 shows the results. The desired trajectory $\mathbf{r}_1^o(t)$ traces the lines connecting points A, B, and C. The translational motion along the trajectory is described by the third-order polynomials with respect to time. The desired trajectory $\mathbf{r}_2^o(t)$ is equal to zero. It is impossible to realize both $\mathbf{r}_1^o(t)$ and $\mathbf{r}_2^o(t)$ for $t = 8 - 12$ s because the second joint is stretched out and the degrees of freedom degenerate. Since pseudoinverse solutions often cause unstable motions near singularities (Nakamura and Hanafusa 1986), the robot manipulator will stop or oscillate before $t = 8$ s if we apply the inverse or pseudoinverse without considering the order of priority. Figure 3 shows that $\mathbf{r}_1^o(t)$ is always satisfied and only $\mathbf{r}_2^o(t)$ is disturbed if both of them are not realizable, which means that the inverse kinematics considering the order of priority is effective for these problems.

$\mathbf{r}_2(t)$ is disturbed at $t = 14$ s because we applied Eq. (7) for the sake of the computational reduction, and it would be reduced if Eq. (6) were applied. In the simulation, the feedback coefficients are chosen as $G_{1,1} = 0$ 1/s, $G_{2,1} = 0$ 1/s², $G_{1,2} = 20$ 1/s and $G_{2,2} = 100$ 1/s².

Fig. 4. 4 d.o.f. manipulator and an obstacle.

Fig. 5. Simulation results for an obstacle avoidance problem. A. Without obstacle. B. With obstacle.

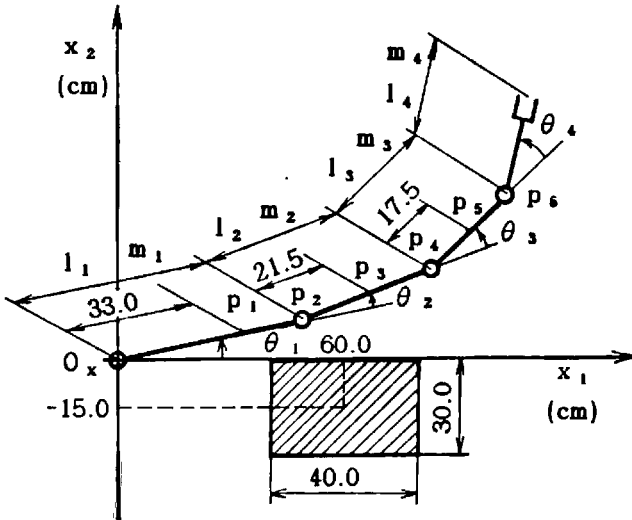


Table 2. Parameters of 4 d.o.f. Manipulator

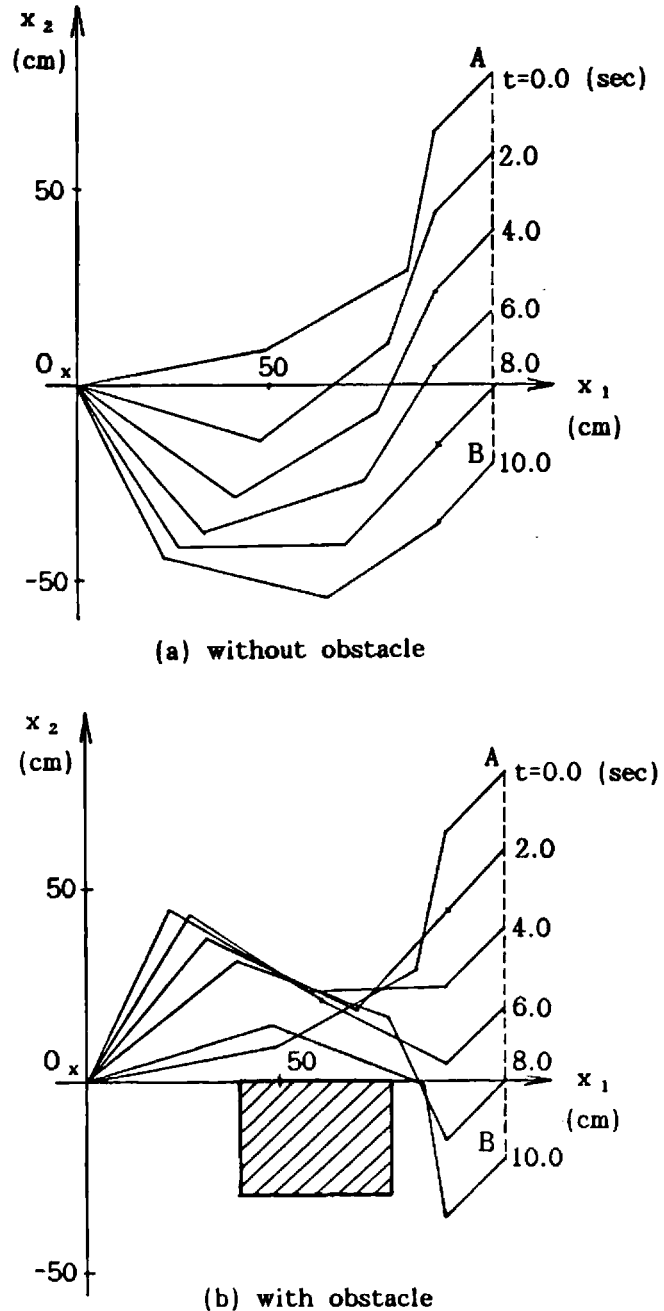
i	l_i (cm)	m_i (kg)	$\theta_{i\max}$ (degree)
1	50.0	30.0	180
2	43.0	25.0	120
3	35.0	20.0	120
4	22.0	10.0	150

4.2. Obstacle Avoidance Using Potential Functions

Now, inverse kinematics based on the order of priority is applied to an obstacle-avoidance problem. Consider a situation where there is a robot manipulator with four degrees of freedom and an obstacle (as shown in Fig. 4). The parameters of the manipulator are summarized in Table 2, where $\theta_{i\max}$ is the limit of the i th joint angle, namely, $|\theta_i| \leq \theta_{i\max}$. The mass of each link is supposed to be uniformly distributed. The manipulator is constrained within a horizontal plane. Therefore, the dynamics is represented by

$$\mathbf{T} = \mathbf{A}(\boldsymbol{\theta})\ddot{\boldsymbol{\theta}} + \mathbf{B}(\boldsymbol{\theta}, \dot{\boldsymbol{\theta}}), \quad (15)$$

where $\mathbf{T}, \boldsymbol{\theta}, \dot{\boldsymbol{\theta}}, \ddot{\boldsymbol{\theta}} \in \mathbb{R}^4$, $\mathbf{A}(\boldsymbol{\theta}) \in \mathbb{R}^{4 \times 4}$ and $\mathbf{B}(\boldsymbol{\theta}, \dot{\boldsymbol{\theta}}) \in \mathbb{R}^4$.



The first manipulation variable $\mathbf{r}_1 \in \mathbb{R}^3$ is described as follows:

$$\mathbf{r}_1 = (x_1 \ x_2 \ \cos(\theta_1 + \theta_2 + \theta_3 + \theta_4))^T. \quad (16)$$

Fig. 6. Distribution of degrees of freedom of UJIBOT, a robot manipulator with 7 d.o.f.

Khatib and Le Maitre (1978) proposed to use artificial potential and dissipative functions in determining the joint torque for obstacle avoidance. According to this method, the joint torque is calculated as follows:

$$\mathbf{T} = -(dP/d\theta + dD/d\dot{\theta})^T, \quad (17)$$

where P and D are artificial potential and dissipative functions, respectively. If the joint torque of Eq. (17) is applied, the following joint acceleration is generated from Eq. (15):

$$\ddot{\theta} = -A^{-1}(\theta)(dP/d\theta + dD/d\dot{\theta})^T + \mathbf{B}(\theta, \dot{\theta}). \quad (18)$$

Now, let us consider the joint acceleration of Eq. (18) as the acceleration of the second manipulation variable. Then, from Eqs. (7), (13), and (18), the joint acceleration considering the first and the second manipulation variables is calculated as follows:

$$\ddot{\theta} = \mathbf{J}_1^* \mathbf{h}_1 - (\mathbf{I} - \mathbf{J}_1^* \mathbf{J}_1) A^{-1}(dP/d\theta + dD/d\dot{\theta})^T + \mathbf{B}. \quad (19)$$

The joint torque to be applied is calculated by substituting θ , $\dot{\theta}$, and Eq. (19) into Eq. (15).

The artificial potential and dissipative functions are defined by

$$P \triangleq P_O + P_J, \quad (20)$$

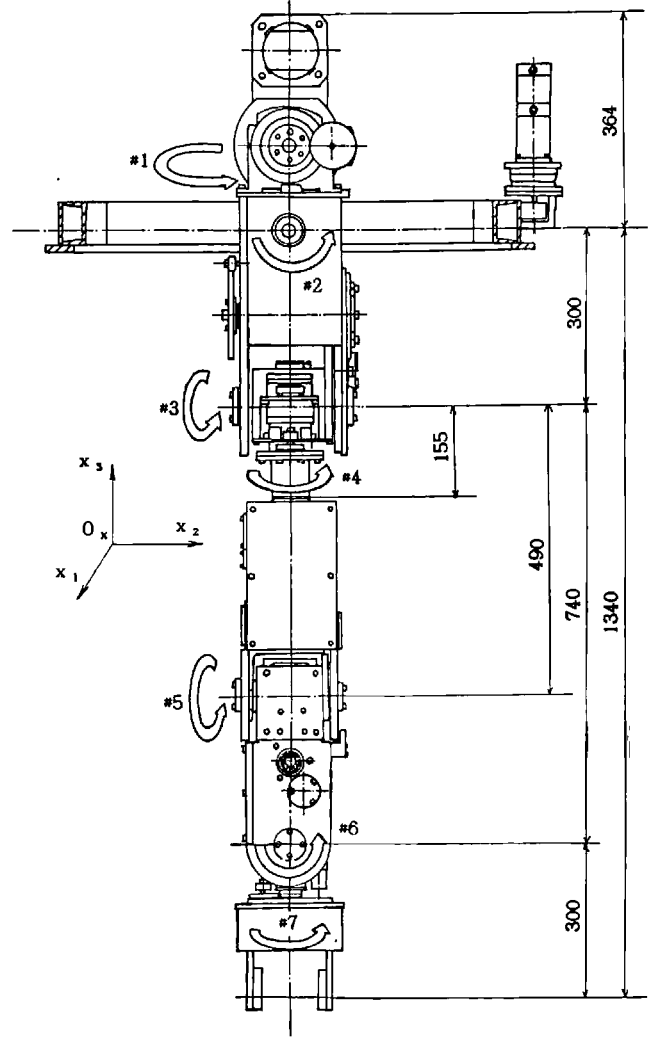
$$P_O \triangleq k_O \sum_{i=1}^6 1/(C_O(\mathbf{p}_i) - 1), \quad (21)$$

$$P_J \triangleq k_J \sum_{i=1}^4 1/(\theta_{i \max}^2 - \theta_i^2), \quad (22)$$

$$D \triangleq k_D \sum_{i=1}^4 \frac{1}{2} \dot{\theta}_i^2, \quad (23)$$

where $\mathbf{p}_i \triangleq (x_{1i}, x_{2i})^T$ (cm) are the positions of points on the manipulator (as shown in Fig. 4) and are used in order to evaluate the distance between the manipulator and the obstacle. $C_O(\mathbf{p}_i)$ is defined by the following equation (Khatib and Le Maitre 1978):

$$C_O(\mathbf{p}_i) \triangleq \left(\frac{x_{1i} - 60}{20} \right)^8 + \left(\frac{x_{2i} + 15}{15} \right)^8, \quad (24)$$



where $C_O(\mathbf{p}_i) = 1$ approximates the contour of the obstacle.

Figure 5 illustrates the results of the numerical simulation. In Fig. 5A, the obstacle does not exist. Figure 5A was computed by neglecting the second term in the right-hand side of Eq. (19). In Fig. 5B, the obstacle is present. The desired trajectory of the first manipulation variable $\mathbf{r}_1(t)$ is the constant velocity motion along the line connecting points A and B . Figure 5B clearly shows that inverse kinematics based on the order of priority is applicable and effective for obstacle avoidance problems. k_O , k_J , and k_D in Eqs. (20)–(23) were

Table 3. Dimensions of UJIBOT

	<i>i</i>	1	2	3	4	5	6	7
	<i>Output</i>	W	35	95	80	64	64	35
<i>M</i>	<i>Rated Voltage</i>	V	24	55	31.3	30.8	30.8	24
<i>o</i>	<i>R.p.m.</i>		3500	1100	4000	4000	4000	3500
<i>t</i>	<i>Torque</i>	nm	9.80×10^{-2}	9.02×10^{-1}	1.96×10^{-1}	1.57×10^{-1}	1.57×10^{-1}	9.80×10^{-2}
<i>o</i>	<i>Inductance</i>	vsec	4.74×10^{-2}	4.54×10^{-1}	6.49×10^{-2}	6.44×10^{-2}	6.44×10^{-2}	4.74×10^{-2}
<i>r</i>	<i>Torque constant</i>	nm/A	4.74×10^{-2}	4.51×10^{-1}	6.47×10^{-2}	6.43×10^{-2}	6.43×10^{-2}	4.70×10^{-2}
	<i>Armature resistance</i>	Ω	1.68	4.7	1.3	1.7	1.7	1.68
	<i>Reduction ratio</i>		3160	2321.4	3703.7	2222.2	2133.3	853.3
	<i>Inertia of motor and transmission</i>	kgm^2	1.444×10^{-4}	1.800×10^{-1}	1.627×10^{-4}	1.098×10^{-4}	1.018×10^{-4}	1.607×10^{-4}
	<i>Mass of link</i>	kg	49.75	43.16	10.79	14.16	13.18	2.29
	<i>Length of link</i>	m	0.0	3.00×10^{-1}	2.781×10^{-1}	2.119×10^{-1}	2.50×10^{-1}	6.853×10^{-2}
<i>Gravity center I_i</i>	<i>l_{i1}</i>	m	-1.856×10^{-2}	3.33×10^{-3}	7.75×10^{-3}	-1.80×10^{-3}	9.82×10^{-3}	0.0
	<i>l_{i2}</i>	m	-3.39×10^{-2}	-2.62×10^{-3}	-1.977×10^{-2}	1.432×10^{-1}	-1.84×10^{-3}	-1.189×10^{-2}
	<i>l_{i3}</i>	m	0.0	-1.427×10^{-2}	3.90×10^{-3}	0.0	8.97×10^{-2}	1.580×10^{-2}
<i>Inertia matrix I_i</i>	<i>l_{i11}</i>	kgm^2	8.374	1.898×10^{-1}	3.119×10^{-2}	2.01×10^{-2}	3.861×10^{-2}	1.03×10^{-3}
	<i>l_{i22}</i>	kgm^2	7.873	1.877×10^{-1}	2.456×10^{-2}	4.089×10^{-2}	1.465×10^{-2}	2.32×10^{-3}
	<i>l_{i33}</i>	kgm^2	9.022×10^{-1}	1.6167	4.303×10^{-2}	2.466×10^{-1}	1.118×10^{-1}	4.40×10^{-3}
	<i>l_{i12}</i>	kgm^2	-1.036×10^{-1}	-3.71×10^{-4}	2.952×10^{-3}	-5.23×10^{-4}	8.79×10^{-4}	0.0
	<i>l_{i23}</i>	kgm^2	-9.79×10^{-2}	-5.284×10^{-3}	5.540×10^{-3}	1.437×10^{-2}	5.476×10^{-3}	3.84×10^{-4}
	<i>l_{i31}</i>	kgm^2	2.007×10^{-1}	-1.622×10^{-2}	4.981×10^{-3}	-4.591×10^{-3}	-5.696×10^{-3}	0.0

chosen as $k_O = 5.0 \times 10^5 \text{ kgcm}^2/\text{s}^2$, $k_J = 6.0 \times 10^4 \text{ kgcm}^2/\text{s}^2$ and $k_D = 1.0 \times 10^4 \text{ kgcm}^2/\text{s}^2$. The feedback coefficients for the first manipulation variable were chosen as $G_{11} = G_{21} = 0$. Concerning the synthesis of the artificial potential field, Khatib (1985) showed that the residual perturbation, which is caused by the potential field to the lower priority task, can be avoided by selecting a contour or a distance behind which the potential field is zero.

5. Experiments

5.1. UJIBOT, a Robot Manipulator with 7 Degrees of Freedom

Figure 6 shows the distribution of degrees of freedom of UJIBOT, a robot manipulator with 7 degrees of

Fig. 7. Overall view of the experimental setup.

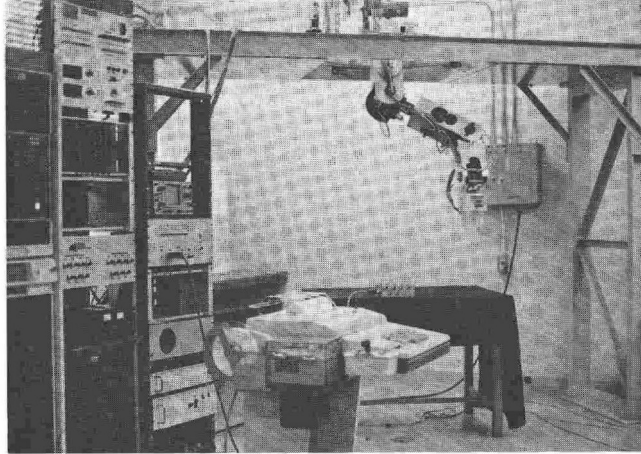


Fig. 8. Reference arm posture θ_r .

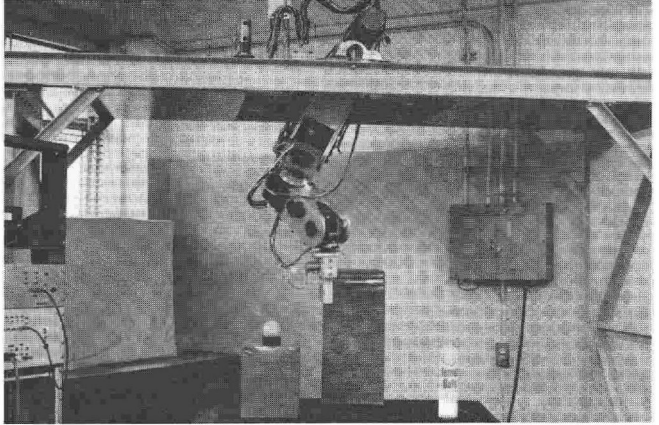


Table 4. Identified Dynamic Characteristics of UJIBOT

<i>i</i>	$P_{Ui} (Vsec^2)$	$Q_{Ui} (Vsec)$	$R_{Ui} (V)$	$S_{Ui} (V/Nm)$
1	3.095	7.034×10^1	6.010×10^{-1}	0
2	6.800	1.812×10^2	3.446×10^{-1}	7.306×10^{-4}
3	2.326	7.060×10^1	2.881×10^{-1}	3.386×10^{-3}
4	1.107	3.905×10^1	2.789×10^{-1}	6.264×10^{-3}
5	1.058	5.506×10^1	3.293×10^{-1}	1.007×10^{-2}
6	4.548	1.962×10^1	5.309×10^{-1}	1.188×10^{-1}
7	3.568×10^{-1}	2.843	5.065×10^{-1}	0

freedom driven by D.C. servo motors. The dimensions of UJIBOT are summarized in Table 3. A gravity center vector \mathbf{l}_i , a vector from the gravity center of the *i*th link to the *i*th joint, and an inertia matrix \mathbf{I}_i are described based on the orthogonal coordinates fixed at the gravity center of the *i*th link, of which three axes are parallel with the corresponding axes of the base Cartesian coordinates when UJIBOT looks as shown in Fig. 6, which means $\theta = 0$.

Since the reduction ratios are large (as shown in Table 3), the inertial, centrifugal, and Coriolis forces of links are negligible in the dynamic characteristics of UJIBOT. Therefore, the approximate dynamics of UJIBOT is represented by

where $\mathbf{V} \in R^7$ is the input voltage vector of motors, $\theta \in R^7$ is the joint variable vector, $\mathbf{C}(\theta) \in R^7$ is the gravity torque vector, $\text{sign } \dot{\theta} \triangleq \text{col.} (\text{sign } \dot{\theta}_i)$ and $\mathbf{P}_U \triangleq \text{diag.} (P_{Ui})$, $\mathbf{Q}_U \triangleq \text{diag.} (Q_{Ui})$, $\mathbf{R}_U \triangleq \text{diag.} (R_{Ui})$, $\mathbf{S}_U \triangleq \text{diag.} (S_{Ui}) \in R^{7 \times 7}$ are the constant matrices whose values are shown in Table 4. Figure 7 shows the overall view of the experimental setup.

5.2. Task Description and Control Scheme

We describe the task as follows: to reach for a tennis ball on a box, grasp it, return it to its initial position, transport the ball along the x_2 -axis at the constant rate of 0.1 m/s for 6.58 s, stop and release the ball into a can below, while avoiding another box that can prevent the motion.

The first and the second manipulation variables are chosen as follows:

$$\mathbf{r}_1 = (x_1 \quad x_2 \quad x_3)^T, \quad (26)$$

$$\mathbf{r}_2 = \theta, \quad (27)$$

where x_1 , x_2 and x_3 are the positions of the end effector. Since the acceleration term is much less than the velocity term in Eq. (25) (see Table 4), velocity control is adopted as the control scheme. The velocity command for the manipulation variable is calculated by

Fig. 9. Motion of UJIBOT without provisions for the obstacle ($G_1 = 3.0 \text{ l/s}$, $G_2 = 0.0 \text{ l/s}$).

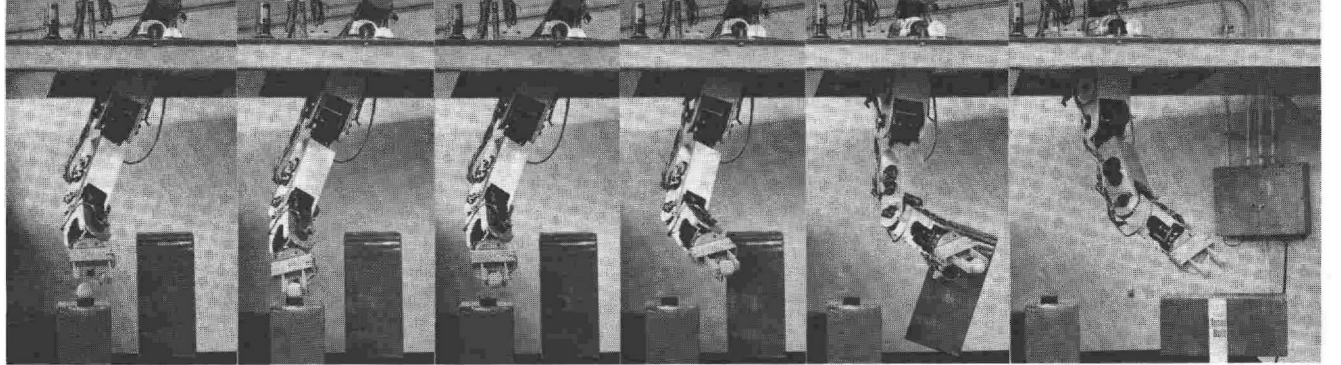
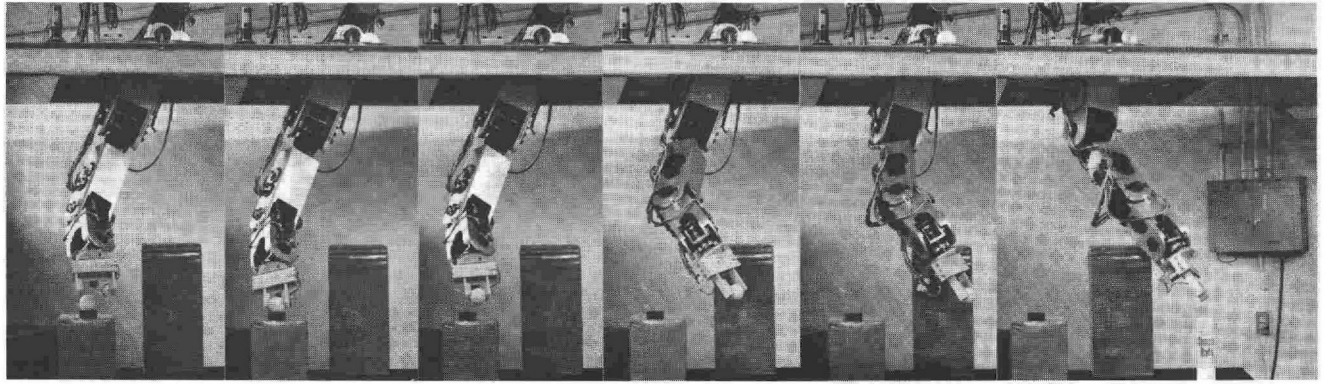


Fig. 10. Motion of UJIBOT with provisions for the obstacle ($G_1 = 3.0 \text{ l/s}$, $G_2 = 0.3 \text{ l/s}$).



$$\dot{\mathbf{r}}_i^* = \dot{\mathbf{r}}_i^o(t) + G_i(\mathbf{r}_i^o(t) - \mathbf{r}_i(t)), \quad (28)$$

where $\dot{\mathbf{r}}_i^*$ is the velocity command for the i th manipulation variable, $\mathbf{r}_i^o(t)$ is the desired trajectory, and G_i is the scalar feedback coefficient. The values of G_i are determined experimentally. The joint velocity command $\dot{\theta}^*$ is calculated according to Eq. (7) as follows:

$$\dot{\theta}^* = \mathbf{J}_1^* \dot{\mathbf{r}}_1^* + (\mathbf{I} - \mathbf{J}_1^* \mathbf{J}_1) \dot{\mathbf{r}}_2^*. \quad (29)$$

The input voltage is determined according to Eq. (25) as follows:

$$\mathbf{V} = \mathbf{Q}_U \dot{\theta}^* + \mathbf{R}_U \operatorname{sign} \dot{\theta}^* + \mathbf{S}_U \mathbf{C}(\theta), \quad (30)$$

where the acceleration term is neglected.

The desired trajectory is represented by the following equations:

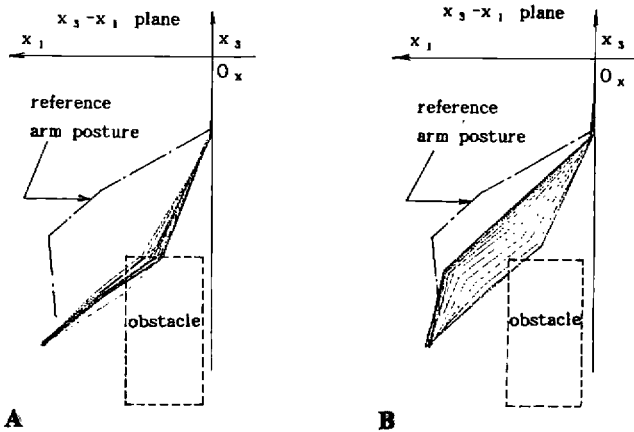
$$\mathbf{r}_1^o(t) = \mathbf{r}_1(t_o) + (t - t_o)(0.0 \quad 0.1 \quad 0.0)^T \text{ (m)}, \quad (31)$$

where $\theta_r \in R^7$ is a constant joint angle, called the *reference arm posture*, which was chosen intuitively so that the elbow of UJIBOT may stay away from the obstacle. Operator intervention of this kind would be a simple but effective method to utilize the global judgment of human operators in obstacle avoidance problems. In the case of complicated obstacles, it would be desirable to choose a time-functional, reference-arm posture. Figure 8 shows the reference-arm posture θ_r .

5.3. Experimental Results and Discussion

Figure 9 shows the motion of UJIBOT when the second term of the right-hand side of Eq. (29) was ne-

Fig. 11. Motion of UJIBOT, projected onto the x_3 - x_1 plane. A. Without provisions for the obstacle ($G_1 = 3.0$ 1/s, $G_2 = 0.0$ 1/s). B. With provisions for the obstacle ($G_1 = 3.0$ 1/s, $G_2 = 0.3$ 1/s).



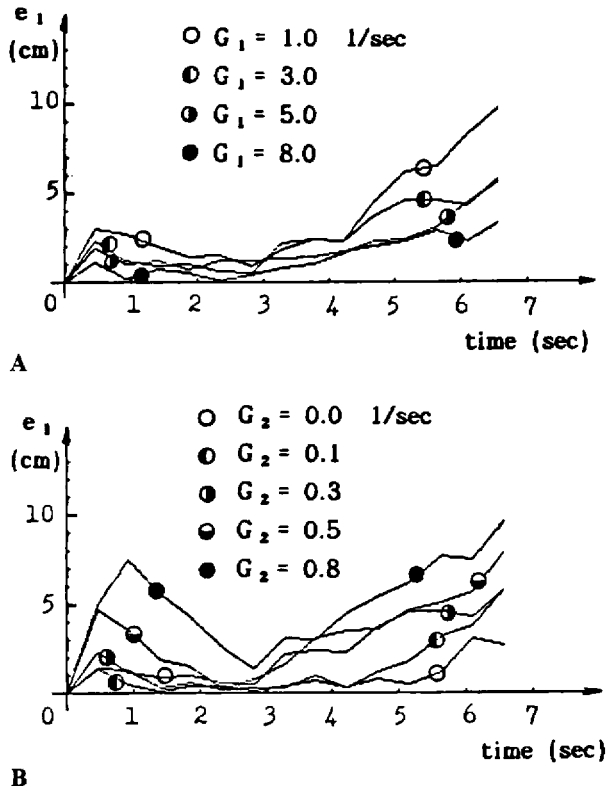
glected: resolved motion rate control according to Whitney (1969). UJIBOT came into collision with the obstacle.

Figure 10 shows the motion of UJIBOT when the second term of Eq. (29) was considered. UJIBOT successfully avoided the collision with the obstacle by utilizing redundancy. Figure 11 shows the motions projected onto the x_3 - x_1 plane every 0.47 s. The chained lines represent the reference-arm posture. The broken lines mean the obstacle. It was found that the elbow of UJIBOT was lifted by the reference-arm posture and avoided the obstacle while the end effector was tracing the given trajectory. These experimental results proved that inverse kinematics based on the order of priority can be implemented in actual control systems for redundant robot manipulators and can be effective in utilizing redundancy. It took 47 ms of sampling time for real-time computation of Eqs. (28)-(30) using a minicomputer NOVA 03 with a floating-point processing unit.

Experiments were also performed to investigate the relationship between the feedback coefficients and the control performance. Figures 12 and 13 show the errors of the first and the second manipulation variables: that is, $e_1 \triangleq \|r_1^o(t) - r_1(t)\|$ and $e_2 \triangleq \|r_2^o - r_2(t)\|$, when G_1 and G_2 changed. From Figs. 12 and 13, the following facts were clarified concerning the feedback coefficients G_1 and G_2 :

1. To increase G_1 as long as it guarantees stability means to reduce e_1 and hardly disturbs e_2 .
2. Having G_2 greater than a certain value is fruitless in improving e_2 .

Fig. 12. Errors of the first manipulation variable, $e_1 = \|r_1^o(t) - r_1(t)\|$. A. G_1 changes, $G_2 = 0.3$ 1/s. B. $G_1 = 3.0$ 1/s, G_2 changes.



3. Increasing G_2 disturbs e_1 to some extent, but this could be overcome by considering a more precise dynamical model.

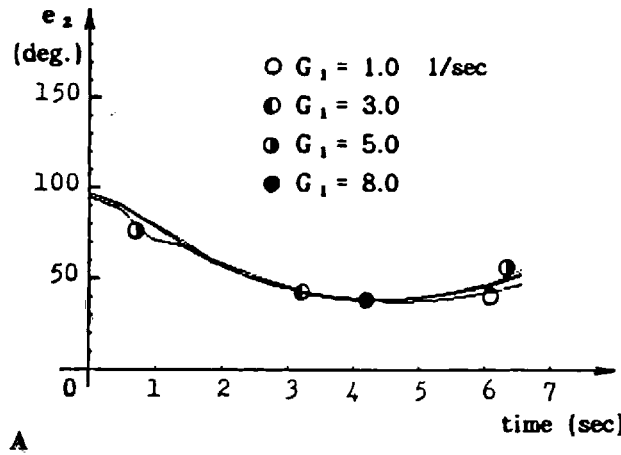
6. Conclusion

The concept of task priority was introduced into the inverse kinematic problem of redundant manipulators, and an inverse kinematic solution was derived taking into account the order of priority, which can be regarded as an instantaneously optimal solution suitable for real-time redundancy control.

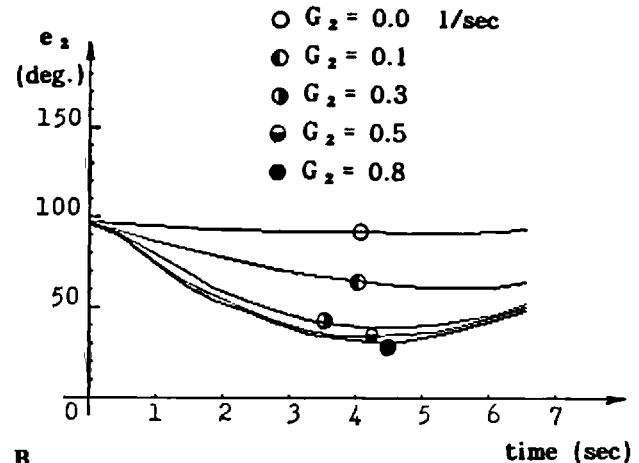
Numerical simulations and experiments were performed in order to verify the effectiveness and the implementation of the solution for redundancy control problems.

We confirmed that dividing a task into subtasks with the order of priority is a remedy for overcoming the degeneracy of degrees of freedom. The obstacle-

Fig. 13. Errors of the second manipulation variable, $e_2 = \|\mathbf{r}_2^o - \mathbf{r}_2(t)\|$. A. G_1 changes, $G_2 = 0.3$ 1/s. B. $G_1 = 3.0$ 1/s, G_2 changes.



A



B

avoidance problem was solved in two ways: (1) the potential functions of obstacles were used to determine the motion of the second manipulation variable, and (2) the reference joint angle intuitively given by an operator was used to determine the motion of the second manipulation variable. Although the first method may be powerful enough for complicated obstacles, it requires an environment model and a great deal of computation. The second method is easier, as it gives the reference information for avoiding obstacles and decreases the computational amount, although it requires the intervention of an operator.

References

- Benati, M., Morasso, P., and Tagliasco, V. 1982. The inverse kinematic problem for anthropomorphic manipulator arms. *J. Dyn. Sys., Meas., Contr.* 104:110–113.
- Boullion, T. L., and Odell, P. L. 1971. *Generalized inverse matrices*. New York: Wiley-Interscience.
- Freund, E. 1977 (Tokyo). Path control for a redundant type of industrial robot. *Proc. 7th Int. Symp. Industr. Robots*, pp. 107–114.
- Hanafusa, H., Yoshikawa, T., and Nakamura, Y. 1978. Control of articulated robot arms with redundancy. *Preprints 21st Joint Automatic Contr. Conf. in Japan*, pp. 237–238. (in Japanese)

- Hanafusa, H., Yoshikawa, T., and Nakamura, Y. 1981 (Kyoto). Analysis and control of articulated robot arms with redundancy. *Preprints 8th Triennial IFAC World Congress* 14:78–83.
- Hanafusa, H., Yoshikawa, T., and Nakamura, Y. 1983. Redundancy analysis of articulated robot arms and its utilization for tasks with priority. *Trans. Society of Instruments and Contr. Engineers* 19:421–426. (in Japanese)
- Khatib, O. 1985 (St. Louis). Real-time obstacle avoidance for manipulators and mobile robots. *Proc. 1985 Int. Conf. Robotics and Automation*, pp. 500–505.
- Khatib, O., and Le Maitre, J.-F. 1978 (Udine, Italy). Dynamic control of manipulators operating in a complex environment. *Proc. 3rd Int. CISM-IFToMM Symp.*, pp. 267–282.
- Klein, C. A. 1984 (Kyoto). Use of redundancy in the design of robotic systems. *Preprints 2nd Int. Symp. Robotics Res.*, pp. 58–66.
- Klein, C. A., and Huang, C. H. 1983. Review of pseudoinverse control for use with kinematically redundant manipulators. *IEEE Trans. Sys., Man, Cyber.* SMC-13:245–250.
- Konstantinov, M. S., Markov, M. D., and Nenchev, D. N. 1981 (Tokyo). Kinematic control of redundant manipulators. *Proc. 11th Int. Symp. Industr. Robots*, pp. 561–568.
- Liegeois, A. 1977. Automatic supervisory control of the configuration and behavior of multibody mechanisms. *IEEE Trans. Sys., Man, Cyber.* SMC-7:868–871.
- Luh, J. Y. S., Walker, M. W., and Paul, R. P. C. 1980. Resolved acceleration control of mechanical manipulators. *IEEE Trans. Automatic Contr.* 25:468–474.
- Maciejewski, A. A., and Klein, C. A. 1985. Obstacle avoidance for kinematically redundant manipulators in dynamically varying environments. *Int. J. Robotics Res.* 4(3):109–117.

-
- Nakamura, Y., and Hanafusa, H. 1986. Inverse kinematic solutions with singularity robustness for robot manipulator control. *J. Dyn. Sys., Meas., Contr.* 108:163–171.
- Nakano, E., and Ozaki, S. 1974 (Tokyo). Cooperative control of a pair of anthropomorphous manipulators—
MELARM. *Proc. 4th Int. Symp. Industr. Robots*, pp.
250–260.
- Uchiyama, M. 1979, Study on dynamic control of artificial arms—part 1. *Trans. Japanese Society of Mechanical Engineers C-45:314–322.* (in Japanese)
- Whitney, D. E. 1969. Resolved motion rate control of manipulators and human prostheses. *IEEE Trans. Man-Machine Sys. MMS-10:47–53.*
- Whitney, D. E. 1972. The mathematics of coordinated control of prostheses and manipulators. *J. Dyn. Sys., Meas., Contr.* 94:303–309.